Definitive Ideal-Gas Thermochemical Functions of the $H_2{}^{16}O$ Molecule

Tibor Furtenbacher and Tamás Szidarovszky
MTA-ELTE Complex Chemical Systems Research Group, H-1117 Budapest, Pázmány Péter sétány 1/A, Hungary

Jan Hrubý
Institute of Thermomechanics of the CAS, v.v.i., Dolejškova 5, Prague 8, CZ-18200, Czech Republic

Aleksandra A. Kyuberis and Nikolai F. Zobov
Institute of Applied Physics, Russian Academy of Science, Ulyanov Street 46, Nizhny Novgorod 603950, Russia

Oleg L. Polyansky and Jonathan Tennyson
Department of Physics and Astronomy, University College London, London WC1E 6BT, United Kingdom

Attila G. Császár[a)]
MTA-ELTE Complex Chemical Systems Research Group, H-1117 Budapest, Pázmány Péter sétány 1/A, Hungary

(Received 11 July 2016; accepted 28 October 2016; published online 15 December 2016)

A much improved temperature-dependent ideal-gas internal partition function, $Q_{\rm int}(T)$, of the $H_2{}^{16}O$ molecule is reported for temperatures between 0 and 6000 K. Determination of $Q_{\rm int}(T)$ is principally based on the direct summation technique involving all accurate experimental energy levels known for $H_2{}^{16}O$ (almost 20 000 rovibrational energies including an almost complete list up to a relative energy of 7500 cm^{-1}), augmented with a less accurate but complete list of first-principles computed rovibrational energy levels up to the first dissociation limit, about 41 000 cm^{-1} (the latter list includes close to one million bound rovibrational energy levels up to $J = 69$, where J is the rotational quantum number). Partition functions are developed for *ortho*- and *para*-$H_2{}^{16}O$ as well as for their equilibrium mixture. Unbound rovibrational states of $H_2{}^{16}O$ above the first dissociation limit are considered using an approximate model treatment. The effect of the excited electronic states on the thermochemical functions is neglected, as their contribution to the thermochemical functions is negligible even at the highest temperatures considered. Based on the high-accuracy $Q_{\rm int}(T)$ and its first two moments, definitive results, in 1 K increments, are obtained for the following thermochemical functions: Gibbs energy, enthalpy, entropy, and isobaric heat capacity. Reliable uncertainties (approximately two standard deviations) are estimated as a function of temperature for each quantity determined. These uncertainties emphasize that the present results are the most accurate ideal-gas thermochemical functions ever produced for $H_2{}^{16}O$. It is recommended that the new value determined for the standard molar enthalpy increment at 298.15 K, 9.904 04 ± 0.000 01 kJ mol^{-1}, should replace the old CODATA datum, 9.905 ± 0.005 kJ mol^{-1}. © *2016 AIP Publishing LLC for the National Institute of Standards and Technology.* [http://dx.doi.org/10.1063/1.4967723]

Key words: bound and unbound states; ideal-gas thermochemical quantities; nuclear motion theory; *ortho*- and *para*-$H_2{}^{16}O$; partition function; water.

CONTENTS

[a)]Author to whom correspondence should be addressed; electronic mail: csaszar@chem.elte.hu.

List of Tables

List of Figures

1. Introduction

Water, the most abundant polyatomic molecule in the universe, plays a major role in the radiative balance of the atmospheres of many astronomical objects, including the atmosphere of our own Earth.[1–3] Water is ubiquitous in cool stellar and substellar (brown dwarf) environments where it is present over a wide range of temperatures including very high ones ($T > 3000$ K), outside the range of most experimental laboratory techniques. Water is also important for models of combustion systems[4,5] at medium to high temperatures (though still less than 3000 K). Predicting high-temperature thermochemical quantities and high-temperature spectra of water is important for understanding many of these environments. The related modeling studies need the accurate knowledge of the partition function, $Q(T)$, of water from the cold to the hot and some other ideal-gas thermochemical functions which can be determined straightforwardly[6] from $Q(T)$.

Due to their considerable scientific and engineering interest, temperature-dependent thermochemical properties of molecular systems such as water have been reported in several databases and information systems.[5,7–19] Most useful for many practical applications would be real-gas and not ideal-gas data,[19] but these are available only for a relatively small number of molecules and they are hard to obtain via theoretical (quantum chemical) approaches. Ideal-gas data, forming the majority of data in the cited information systems, are considerably more straightforward to obtain theoretically. As emphasized in standard textbooks,[6,20,21] all ideal-gas temperature-dependent thermochemical functions can be derived from the partition function and its moments. It would be preferable to obtain accurate temperature-dependent thermochemical functions experimentally. However, even in the few cases and temperature ranges where this is available it is built upon effective (anharmonic) spectroscopic quantities, which puts a considerable constraint on the accuracy that can be expected from such studies, especially at elevated temperatures. To accommodate the full temperature range required by the applications, one must rely on some sort of computation in order to derive the ideal-gas partition and thermochemical functions.

It is important to point out that ideal-gas thermochemistry has been developed with an emphasis on chemical reactions; thus, only those effects have been considered important which readily change during a usual chemical reaction. A consequence, as noted by Ruscic,[19] is that "practical *thermochemical* functions ignore the overall nuclear spin contribution... as well as the isotope mixing component, which, in any stoichiometrically balanced chemical reaction, cancel out

across the involved chemical species." In spectroscopy, in scientific and engineering applications requiring line-by-line data, and when treating systems out of equilibrium (see, e.g., Ref. 22), partition functions and thermochemical functions containing nuclear-spin contributions may be needed. Thus, in this paper we do consider nuclear spins in our treatment and compute thermochemical quantities for *ortho*- and *para*-$H_2{}^{16}O$, as well as for their nuclear-spin-equilibrated mixture. Treatment of the state-independent degeneracy factor is made simple here by the fact that the nonpermuting ^{16}O nucleus has zero nuclear spin.

For many semirigid molecules, the simplest analytic technique[21,23] to obtain internal partition functions, namely use of the harmonic oscillator (HO) and rigid rotor (RR) approximations for the vibrational and the rotational motions, respectively, yields reasonably accurate results at relatively low temperatures (especially around room temperature). Partition functions have an integrative nature: they can be considered as a direct sum of weighted energy levels. This provides much room for approximate treatments; for example, an approach more sophisticated than the RRHO approximation uses effective spectroscopic Hamiltonians providing a much improved estimate for the partition functions and the related thermochemical data, even up to somewhat elevated temperatures.[24–26] For water, the perturbative approach is insufficient and even breaks down at relatively low excitations or, alternatively, at relatively low temperatures. Therefore, to obtain highly accurate high-temperature partition and thermodynamic functions for the water isotopologues requires the use of variational techniques during the computation of the energy levels.[27]

A considerable volume of knowledge has been accumulated about computing thermochemical functions for $H_2{}^{16}O$. Important developments on the computational front include studies by Martin *et al.*,[28] Harris *et al.*,[29] Vidler and Tennyson (VT),[30] and others.[19,31–33] Two major sources of high-quality thermochemical data are JANAF (Joint Army–Navy–Air Force)[15] and Gurvich,[11,34] which were originally set up to supply, after appropriate compilation and evaluation, thermochemical data for modeling the thermochemistry of a large number of small and medium-sized chemical systems. For the presentation of the results of this study, the JANAF standard is followed: the JANAF-style tables list energy functions, entropies, enthalpies, and heat capacities as a function of temperature up to 6000 K. The JANAF tables themselves list thermochemical functions from 100 K with 100 K increments, but in the present study, due to the high experimental spectroscopic accuracy of our lower energy levels, we can list meaningful thermochemical quantities at even lower temperatures. Furthermore, in the supplementary material[35] to this paper the thermochemical quantities are listed at 1 K intervals to ensure that future interpolation efforts could retain the high accuracy of the present study. Furthermore, the International Association for the Properties of Water and Steam (IAPWS),[16] an expected user of the data supplied here, requires thermodynamic data tabulated with this fine granularity.

Our data, with the associated approximately two standard deviation uncertainties, should be considered as the most accurate ideal-gas thermochemical data available for $H_2{}^{16}O$. There are several facets of the present study supporting this statement. Prior to the PoKaZaTeL data[36] used in the present study (*vide infra*), the most complete *ab initio* database for $H_2{}^{16}O$ energy levels and transitions was the so-called BT2 line list,[37] which contains 221 097 energy levels (up to $J = 50$ and $E \leq 30\,000$ cm^{-1}) and half a billion transitions. The high-accuracy first-principles PoKaZaTeL dataset employed in this study is complete up to the first dissociation limit and contains four times more, close to one million energy levels. Prior to the present work, the most reliable partition sum and related thermochemical data was due to VT.[30] VT used a hybrid approach similar to the one employed here, but one which was necessarily more approximate. They summed over the then available empirical energy levels,[38] augmented with levels from a variational line list computed by Viti,[39,40] and then completed it with predicted band origins to dissociation[41] combined with a very approximate treatment of rotation. All sums were simply truncated at the dissociation limit which was assumed to be 41 088 cm^{-1}; any states lying above this limit were ignored. The present study utilizes a much larger set of experimental energy levels and a much larger set of computed first-principles energy levels than any of the previous studies.

Due to the Boltzmann distribution characterizing thermodynamic equilibria, the contribution of energy levels to the partition function depends strongly on the thermodynamic temperature T of the system. At the lowest temperatures, where the thermochemical functions depend only on a relatively small number of energy levels, an accuracy considerably higher than that provided by even the most sophisticated modeling studies can be achieved, once energy levels of experimental quality are used. At the lowest temperatures, one must also be careful how the *ortho* and *para* nuclear-spin isomers of $H_2{}^{16}O$ are treated.[22] These isomers are treated explicitly during the present study.

Given the high accuracy we aim at in this study up to very high temperatures, one must investigate not only the contribution of bound rovibrational states on the ground electronic state to the thermochemical functions, but also those of resonance states and higher electronic states. As shown recently for the case of three isotopologues of the diatomic molecule MgH,[42] beyond a given temperature, dependent upon the first dissociation threshold of the molecule, unbound states can make a significant contribution to the partition function and the related thermochemical quantities. Studies have begun to consider quasibound states of water,[43,44] and in this paper such molecular states are considered for the partition function of water for the first time, albeit via a very simple model.

In a complete treatment, the contribution of excited electronic states must also be investigated. The effect of the excited electronic states of $H_2{}^{16}O$ has not been considered during the present study, as it was deemed to be minuscule even at the high accuracy sought in this study.

Finally, we note that many of the modeling methods of the present investigation on $H_2{}^{16}O$ can be utilized when determining temperature-dependent thermochemical functions of other molecular systems.

2. Methodological Details

The total partition function is assumed to be the product of the internal and the translational partition functions. The bound rovibrational energy levels used for computing the ideal-gas internal partition function, $Q_{\text{int}}(T)$, of $H_2{}^{16}O$ come from two sources: a measured active rotational–vibrational energy levels (MARVEL)[45–47] analysis of all the available experimental transitions,[48] and a recent first-principles computation, utilizing the PoKaZaTeL potential energy surface (PES),[36] of all the bound rovibrational states on the ground electronic state of $H_2{}^{16}O$. These two sources will be described separately, followed by a discussion of the computation of the thermochemical functions. Since it is important to understand the accuracy of all the computed thermochemical quantities, an error and uncertainty analysis is also performed as part of this section.

2.1. MARVEL energy levels

The most accurate source of bound rovibrational energy levels of $H_2{}^{16}O$ is the MARVEL database, obtained as part of an IUPAC-sponsored research effort.[48–52] The MARVEL process[46] involves a weighted least-squares algorithm, whereby first a spectroscopic network (SN)[53] is built from the experimentally observed and assigned (labeled) spectral transitions, involving all available sources of data, and then the transitions, based on the Ritz principle, are inverted to determine experimental-quality (MARVEL) energy levels. Each transition has a label for the upper and lower states between which the transition occurs. The labeling scheme for $H_2{}^{16}O$ uses six quantum numbers: the approximate normal-mode quantum numbers v_1, v_2, and v_3 describe the vibrations (symmetric stretch, bend, and antisymmetric stretch, respectively), and the usual exact J rotational quantum number and the approximate K_a and K_c values are used for the description of the rotational excitation.[54]

The MARVEL database[48] for $H_2{}^{16}O$ contains 18 486 energy levels, all the known and validated experimentally determined bound rotational–vibrational energy levels of $H_2{}^{16}O$ prior to 2013. The uncertainty of the MARVEL energy levels is between 10^{-6} and 10^{-2} cm^{-1}; each energy level carries its own uncertainty. Even with the MARVEL database at hand, complete in rovibrational energies up to about 7500 cm^{-1}, one must realize that for higher temperatures (above about 600 K) there are insufficient observed rovibrational energy levels available to converge the partition function of $H_2{}^{16}O$ to 10^{-4}% accuracy, the characteristic accuracy below 600 K. Therefore, if accurate thermochemical functions are needed at higher temperatures one must substantially augment the experimental (MARVEL) set of rovibrational energy levels. In the fourth age of quantum chemistry,[55] the best way to achieve this is through the use of results from first-principles nuclear motion computations, employing an exact nuclear kinetic energy operator and a highly accurate adiabatic global PES.[27,56]

2.2. First-principles energy levels

Following this recommendation, in this study the MARVEL energy levels are augmented for the bound states by first-principles energy levels. The first-principles bound rovibrational energy levels used during this study are taken from a database called PoKaZaTeL.[36]

The PoKaZaTeL energy levels were computed using a global, adiabatic, empirically adjusted PES[36] and the DVR3D nuclear-motion code.[57] This data set contains 810 252 energy levels up to the first dissociation limit [D_0 = 41 145.94(12) cm^{-1}],[58] and it extends all the way to J = 69. As a result, the PoKaZaTeL set represents all the bound rovibrational energy levels of $H_2{}^{16}O$.

2.3. The hybrid database

The most accurate and most complete database of bound rovibrational energy levels of $H_2{}^{16}O$ can be obtained by combining the complete PoKaZaTeL database with the accurate MARVEL database. Therefore, we replaced the PoKaZaTeL energy levels with MARVEL energies whenever possible and in this way we obtain what is called hereafter the hybrid database.

For quantification of the approximately two standard deviation uncertainties of the computed thermochemical quantities, it is essential that each energy level has its own uncertainty. The experimental MARVEL energy levels have well determined uncertainties, originating from the uncertainties of the measured transitions. The computed PoKaZaTeL list does not have associated uncertainties. However, by comparing the PoKaZaTeL and MARVEL energy levels, when both are available, we could estimate the average uncertainties of the PoKaZaTeL energy levels. Finally, up to 20 000 cm^{-1} a value 0.2 cm^{-1} was taken for these one standard deviation uncertainties, while above this energy a conservative estimate of 0.5 cm^{-1} was assumed.

2.4. Thermochemical quantities

The internal partition function of a free molecule, Q_{int}, and its first two moments, Q'_{int} and Q''_{int}, can be written as[6,28,33]

$$Q_{\text{int}} = \sum_i g_i(2J_i + 1)\exp\left(\frac{-c_2E_i}{T}\right), \tag{1}$$

$$Q'_{\text{int}} = \sum_i g_i(2J_i + 1)\left(\frac{c_2E_i}{T}\right)\exp\left(\frac{-c_2E_i}{T}\right), \tag{2}$$

$$Q''_{\text{int}} = \sum_i g_i(2J_i + 1)\left(\frac{c_2E_i}{T}\right)^2\exp\left(\frac{-c_2E_i}{T}\right), \tag{3}$$

where $c_2 = hc/k_B$ is the second radiation constant (the numerical values of the constants employed in this study are given in Table 1), J_i is the rotational quantum number, E_i is the rotational–vibrational energy level given in cm^{-1}, T is the thermodynamic temperature in K, g_i is the nuclear spin degeneracy factor (representing both state-dependent and state-independent elements), and the index i runs over all possible rovibronic energies considered. In the case of $H_2{}^{16}O$, the values of g_i are taken as 3 for the *ortho* and 1 for the *para* nuclear-spin states, in accord with the HITRAN convention.[17]

TABLE 1. Physical constants employed in this study

Name	Value	Reference
Second radiation constant, c_2	1.438 777 36(83) cm K	59
Molar gas constant, R	8.314 459 8(48) J mol^{-1} K^{-1}	59
Avogadro constant, N_A	6.022 140 857(74) $\times 10^{23}$ mol^{-1}	59
Planck constant, h	6.626 070 040(81) $\times 10^{-34}$ J s	59
Boltzmann constant, k_B	1.380 648 52(79) $\times 10^{-23}$ J K^{-1}	59
$H_2{}^{16}O$ molecular mass, m	2.990 724 580(36) $\times 10^{-26}$ kg	60

The full partition function Q of a molecule in the ideal gas state is a product of the internal partition function, $Q_{\rm int}$, and the translational partition function, $Q_{\rm trans}$. The latter can be expressed as[21]

$$Q_{\rm trans} = V\Lambda^{-3}, \tag{4}$$

where V is the volume of the system, $\Lambda = h/(2\pi m k_B T)^{1/2}$ is the de Broglie wavelength, h is the Planck constant, and m is the molecular mass (the numerical values of the constants are given in Table 1).

The Helmholtz energy A, the internal energy minus the product of thermodynamic temperature and entropy, is obtained from its fundamental relation to the canonical partition function Q, namely

$$A = -RT\ln Q = -RT\ln Q_{\rm int} - RT\ln\frac{V}{\Lambda^3}, \tag{5}$$

where R denotes the molar gas constant (Table 1). All thermochemical functions can then be derived using thermodynamic identities; in particular,

$$p = -\frac{\partial A}{\partial V}, \quad S = -\frac{\partial A}{\partial T}, \quad G = A + pV, \quad H = G + TS, \tag{6}$$

where p, S, G, and H are pressure, entropy, Gibbs energy, and enthalpy, respectively. The first relation obviously results in the ideal gas equation of state, $pV = RT$. The isochoric heat capacity is obtained as

$$C_v = T\frac{\partial S}{\partial T} = -T\frac{\partial^2 A}{\partial T^2}, \tag{7}$$

and the isobaric heat capacity of the ideal gas is then $C_p = C_v + R$. All these properties can be obtained using the internal partition function, Eq. (1), and its first two moments, Eqs. (2) and (3). The most important and widely used thermochemical functions can be constructed as follows:

(a) The standardized enthalpy is

$$H(T) - H(298.15) = RT\frac{Q'_{\rm int}}{Q_{\rm int}} + \frac{5}{2}RT - H(298.15), \tag{8}$$

where $H(298.15)$ is the (absolute) enthalpy at the reference temperature taken to be 298.15 K.

(b) The Gibbs energy function is

$$\begin{aligned}\text{gef}(T,p) &= -\frac{G(T) - H(298.15)}{T} \\ &= R\ln Q_{\rm int} + R\ln\frac{(2\pi m)^{3/2}(k_B T)^{5/2}}{h^3 p} + \frac{H(298.15)}{T}.\end{aligned} \tag{9}$$

(c) The entropy is

$$S(T,p) = R\frac{Q'_{\rm int}}{Q_{\rm int}} + R\ln Q_{\rm int} + \frac{5}{2}R + R\ln\frac{(2\pi m)^{3/2}(k_B T)^{5/2}}{h^3 p}. \tag{10}$$

(d) The isobaric heat capacity is

$$C_p(T) = R\left[\frac{Q''_{\rm int}}{Q_{\rm int}} - \left(\frac{Q'_{\rm int}}{Q_{\rm int}}\right)^2\right] + \frac{5}{2}R. \tag{11}$$

As seen in Table 1, the physical constants used in Eqs. (1)–(11), similarly to the energy levels, have well defined uncertainties. The uncertainties of the c_2 and R constants are rather substantial, in fact larger than the relative uncertainties of many of the MARVEL energy levels. Since c_2 appears alongside the E_i energies in Eqs. (1)–(3), its uncertainty has a significant effect on the uncertainties of the computed thermochemical functions (*vide infra*).

2.5. The effect of unbound states on the thermochemical properties of water

A possible route to determine the $Q_U(T)$ contribution of the unbound molecular rovibrational states to the partition function $Q_{\rm int}(T)$ of water is through the use of the expression

$$Q_U(T) = \int_0^\infty \rho_U(E)\exp(-\beta E)\mathrm{d}E, \tag{12}$$

where $\rho_U(E)$ is the density of the unbound rovibrational states for $H_2{}^{16}O$ and $\beta = 1/k_B T$. In the present work, a simple model is used to evaluate Eq. (12): the unbound (scattering/continuum) states of the $H_2{}^{16}O$ system are approximated as the eigenstates of the noninteracting bound OH radical and an OH + H scattering system, in which the OH is treated as a particle with no internal degrees of freedom. The density of states for the OH radical can be given by

$$\rho^{(\rm OH)}(E) = \sum_{l,v}(2l+1)\delta\left(E - E^{(\rm OH)}_{l,v}\right), \tag{13}$$

while for the OH + H scattering system it is

$$\rho_U^{(\rm OH+H)}(E) = \frac{1}{\pi}\sum_j (2j+1)\frac{\mathrm{d}\eta_j(E)}{\mathrm{d}E}, \tag{14}$$

where l and v are the rotational and vibrational quantum numbers of the OH radical, respectively, j is the rotational quantum number of the H + OH scattering system in the center-of-mass frame, and $\eta_j(E)$ is the scattering phase shift corresponding to a given j.

Applying the formula, motivated by the probability density distribution formula for the sum of two independent random variables,

$$\rho_U(E) = \int_0^\infty \rho^{(\rm OH)}(E')\rho_U^{(\rm OH+H)}(E - E')\mathrm{d}E', \tag{15}$$

for the total density of states, and from combining Eqs. (12)–(15) and utilizing the fact that $\eta_j(E)$ is zero for

$E < D_0$, one obtains

$$Q_{\mathrm{U}}(T) = \left(\sum_{l,v} (2l+1) \exp\left(-\beta E_{l,v}^{(\mathrm{OH})} \right) \right) \left(\frac{1}{\pi} \sum_{j} (2j+1) \int_{D_0}^{\infty} \frac{\mathrm{d}\eta_j(E')}{\mathrm{d}E'} \exp\left(-\beta E' \right) \mathrm{d}E' \right) = Q^{(\mathrm{OH})}(T) Q_{\mathrm{U}}^{(\mathrm{OH+H})}(T). \quad (16)$$

Thus, the total partition function is a product of the partition functions of the noninteracting subsystems, as expected. The final $Q_{\mathrm{U}}(T)$ values were obtained for *ortho*- and *para*-$H_2{}^{16}O$ by multiplying the results of Eq. (16) by 3 and 1, respectively.

The potential energy curves (PEC) for the OH radical and the OH + H system were obtained from the global $H_2{}^{16}O$ PES of Refs. 27 and 56. The OH PEC was simply obtained by setting the second H to a 30 a_0 distance from the OH center-of-mass, while for the OH + H system the PEC was obtained by "relaxing" the orientation of the OH and the OH distance, within 0–3 a_0, for each fixed OH–H distance. Eigenenergies for the OH radical in Eq. (15) were obtained by solving the diatomic rovibrational time-independent Schrödinger equation using 250 spherical-oscillator DVR basis functions[61] with $R_{\mathrm{max}} = 15$ a_0. As in previous studies,[42,62,63] the scattering phase shifts in Eq. (14) were computed using a semiclassical WKB approximation. The maximum j value used in Eq. (14) is 278.

2.6. Uncertainty and error analysis

The exact values of the internal partition functions of molecules are unknown, and thus there are no true reference values available for comparison with the approximate values. Nevertheless, in a computational study claiming high accuracy a quantification of uncertainties must be performed.[64]

There are a few sources of error preventing the determination of "exact" values of $Q_{\mathrm{int}}(T)$. Traditionally, the largest source of the uncertainty in a partition function, especially at higher temperatures, has been the uncertainty about the number of bound energy levels (uncertainty about the energy level density). A second significant source of error lies in the uncertainty of the energy levels used to determine $Q_{\mathrm{int}}(T)$. A third type of (usually less significant) uncertainty is connected with the question of how unbound states and states associated with excited electronic states should be accounted for. A fourth source of uncertainty, so far left unexplored in computational thermochemical studies, is connected to the uncertainty of the physical constants entering Eqs. (1)–(16) (Table 1).

Checking the convergence of partition functions is hard, since Q_{int} grows monotonically as more and more bound energy levels are considered in the direct sum. At low temperatures ($T < 1000$ K), relatively few energy levels are sufficient to reach a converged Q_{int} value (in our definition this means that adding more and more higher-lying energy levels to the sum in Eq. (1) causes only a negligible change, (much) less than 0.01%).

Two simple methods can be used for obtaining the second type of uncertainty mentioned about the partition function and the associated thermochemical quantities: in method A the common error propagation formula is employed, while method B increases and reduces the energy levels by their uncertainties, the two extrema of the given thermochemical function can be calculated and the difference of these extrema provides an uncertainty estimate.

The third type of uncertainty of $Q_{\mathrm{int}}(T)$ comes from the unbound states but, to the best of our knowledge, this uncertainty has not been taken properly into account for molecules containing more than two atoms. Part of the reason is that unbound states start playing a significant role at higher temperatures and only for molecules with a comparatively low dissociation energy. In this work, the effect of unbound states is approximated using the model described in the Sec. 2.5. In the case of bound states, where very accurate reference data are available, the accuracy of the crude "noninteracting OH plus OH + H" model for computing thermodynamic properties can be tested. In fact, this model overestimates the bound-state partition function by a factor of around two. This huge discrepancy is probably due to the fact that the model allows for quantum states with large overlaps between the hydrogen nuclei, which in a more realistic simulation would lead to very high (even unbound) energies and much smaller contributions to the partition function. The situation is expected to be similar in the case of unbound states, that is, the model defined in Sec. 2.5 is expected to overestimate the contribution of the unbound states in the partition function. Thus, taking the computed values of the contribution of unbound states themselves as the uncertainties originating from the unbound states seems to be a safe, conservative estimate.

In the present case of $H_2{}^{16}O$, the hybrid database contains all the existing bound rovibrational energy levels. Completeness of the set of hybrid energy levels may not be maintained perfectly just slightly below the first dissociation limit, where hard-to-determine long-range states may exist;[61,65] therefore, it is worth checking the convergence of $Q_{\mathrm{int}}(T)$ by increasing the number of energy levels considered in the direct sum via moving an E_{cut} cutoff energy value closer and closer to the dissociation limit. Figure 1 illustrates the effect of the increase of E_{cut} on the partition sum at different temperatures. It can be seen that, while at 1000 K the partition sum is fully converged with an E_{cut} of about 8000 cm^{-1}, at 6000 K $Q_{\mathrm{int}}(T)$ does not reach full convergence even at $E_{\mathrm{cut}} = D_0$, so adding new (high-lying) energy levels to the direct sum the value of the partition function might still change noticeably.

To help elucidate the results of Fig. 1, the solid lines in Fig. 2 show the difference, in %, between $Q_{\mathrm{int}}^{\mathrm{tot}}$ (considering all energy levels) and Q_{int}^{39000}, Q_{int}^{40000}, and Q_{int}^{41000} (i.e., considering the energy levels up to $E_{\mathrm{cut}} = 39\,000$, 40 000, and 41 000 cm^{-1}, respectively) as a function of temperature. It can be seen that (a) at 4000 K the differences are still very close to zero and (b) at 6000 K the difference between $Q_{\mathrm{int}}^{\mathrm{tot}}$ and Q_{int}^{41000} is about 0.05%. The dashed lines in the left panel of Fig. 2 show the similar differences for Q''_{int}. It can be seen that at 6000 K the error of $Q''^{41000}_{\mathrm{int}}$ is about 0.3%. Considering that there are almost 13 000 energy levels between 41 000 cm^{-1} and the

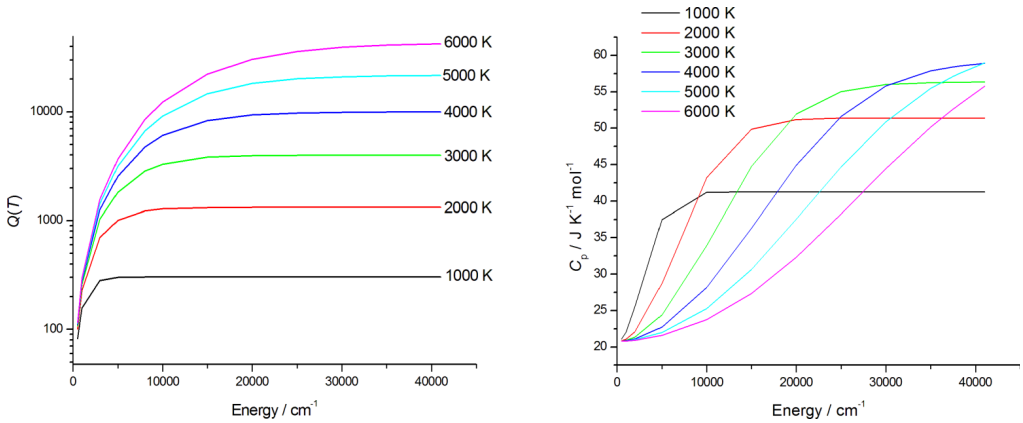

FIG. 1. Left panel: Convergence of the internal partition function $Q_{\rm int}\,(T)$ of $H_2{}^{16}O$ at different temperatures as a function of the energy cutoff value considered in the direct sum (see text). Right panel: Similar curves for the isobaric heat capacity $C_p(T)$ of $H_2{}^{16}O$.

first dissociation limit, and that this number probably grossly overestimates the number of energy levels that sophisticated first-principles computations can miss, we associate the differences of the $Q_{\rm int}^{\rm tot}$ and $Q_{\rm int}^{41000}$ values with the uncertainty which comes from the lack of a truly complete set of bound rovibronic energy levels. Figure 2 also shows why it is so important to determine all rovibrational energy levels up to the dissociation limit. At higher temperatures ($T > 3000$ K), the lack of rovibrational energy levels at the highest level density regions close to dissociation causes significant errors, especially in the cases of Q'' and C_p.

Figure 3 shows errors, in %, which come from the uncertainties of the energy levels. Most importantly, both methods A and B, see above, result in similar, relatively small errors (less than 0.004% in the case of $Q_{\rm int}$ and less than 0.05% in the case of Q''). C_p is the thermochemical quantity most sensitive to uncertainties of energy levels; therefore, the above analysis was repeated for C_p (see the right panels of Figs. 1 and 2).

Figure 4 shows the error contribution of unbound states. It can be seen that (a) up to 4000 K the contribution is very close to zero and (b) at 6000 K the contribution is 3.2% to $Q''_{\rm int}(T)$ and 4.0% to C_p.

There is one more source of error which might influence the final uncertainty of the partition function: the uncertainties of the physical constants. This type of uncertainty is usually negligible, for example, in case of the heat capacity the uncertainty of the molar gas constant is two orders of magnitude less than the other errors and since R is a simple scale factor its uncertainty is negligible. However, in the case of c_2, the second radiation constant, which is the scale factor of energy levels and is inside the sum, the uncertainty of c_2 is not negligible. Figure 5 shows the effect of an assumed error of c_2. It can be seen that below about 2500 K the uncertainty of c_2 determines the final uncertainty of the partition function. Above this temperature, the uncertainty contribution of unbound states dominates. The final uncertainty of the partition function is given by the four uncertainties just described.

3. Results and Discussion

The Q, Q', and Q'' results of *ortho*- and *para*-$H_2{}^{16}O$, along with the nuclear-spin-equilibrated mixture, are presented in Table 2 in 100 K intervals up to 6000 K, starting at 100 K. Table 3 contains three thermochemical functions, $C_p(T)$,

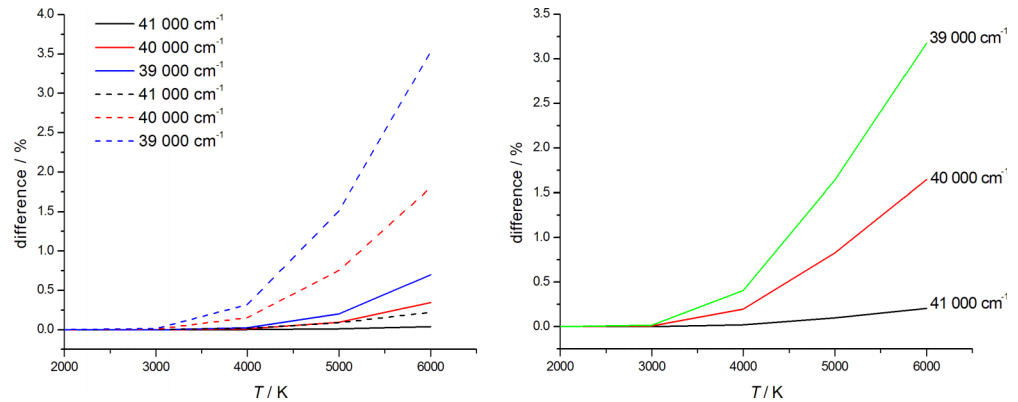

FIG. 2. Left panel: Convergence characteristics of the internal partition function, $Q_{\rm int}\,(T)$ (solid lines), and the second moment of $Q_{\rm int}\,(T)$, $Q''_{\rm int}\,(T)$ (dashed lines), of $H_2{}^{16}O$ utilizing larger and larger sets of energy levels, as a function of temperature, with energy cutoff values given in the inset of the figure. Right panel: Similar curves for the isobaric heat capacity $C_p(T)$ of $H_2{}^{16}O$.

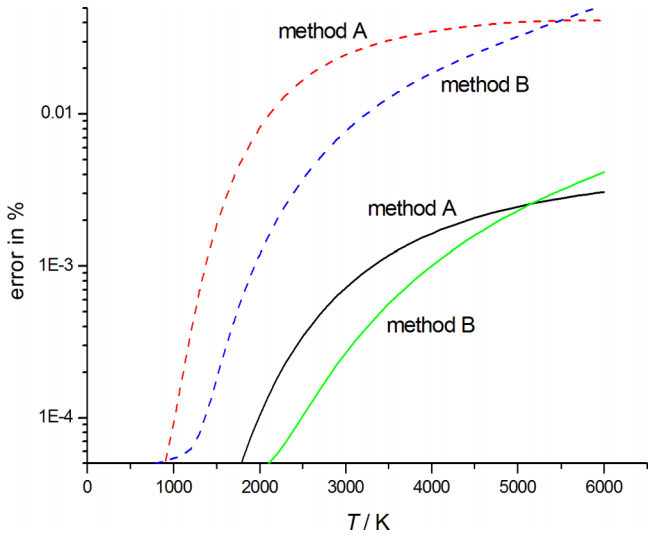

FIG. 3. Error of the partition function (solid lines) and its second moment (dashed lines) using the propagation formula method, Method A, and the "two extrema" method, Method B.

$S(T)$, and $H(T)$, as a function of temperature, as well as their comparison with the best previous results obtained by Ruscic[19] and VT.[30] Note that only the traditional, nuclear-spin-equilibrated thermochemical quantities are compared with literature data in Table 3. The complete set of results at 1 K increments is given in the supplementary material[35] to this paper. Table 4 lists the coefficients of a least-squares fit to our computed partition function, using the traditional form of[30]

$$\ln Q_{\text{int}} = \sum_{i=0}^{6} a_i (\ln T)^i. \tag{17}$$

In order to get the best reproduction of the directly computed values, the fit had to be performed in two separate temperature ranges. The first range is 0–200 K, the other is 201–6000 K. These fits can reproduce, in both regions, the values of $\ln Q_{\text{int}}$ reasonably accurately, within about 0.1%. Nevertheless, as

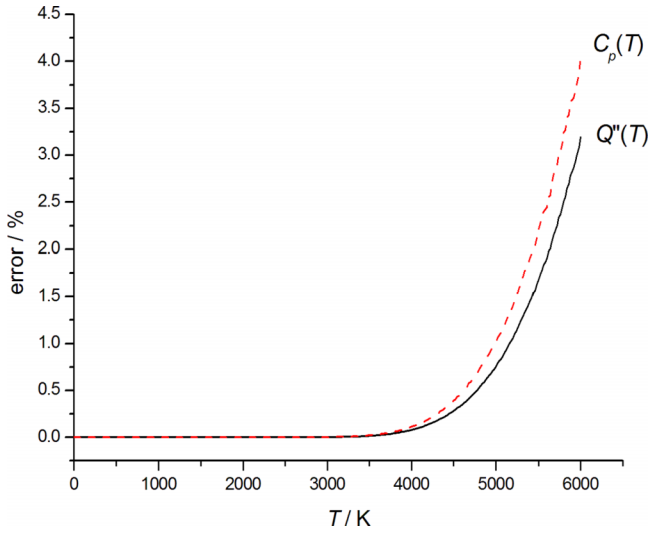

FIG. 4. Error due to the neglect of the unbound states during the determination of $Q''_{\text{int}}(T)$ (solid line) and $C_p(T)$ (dashed line).

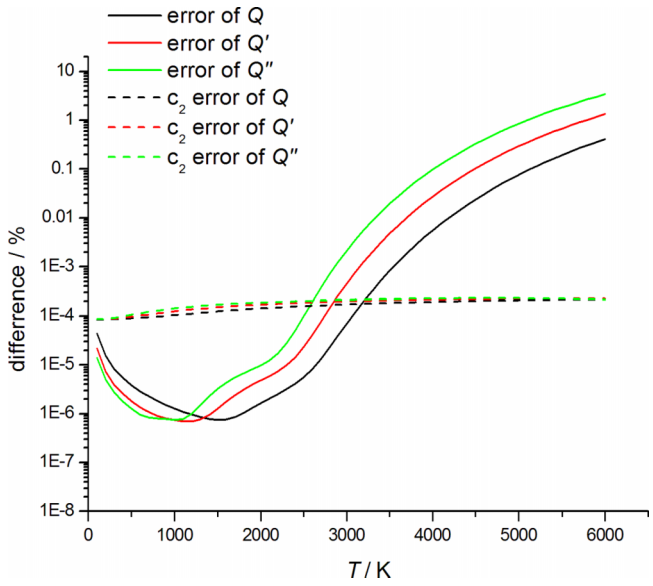

FIG. 5. Error contribution of energy levels (solid lines) and the error contribution of the uncertainty of the second radiation constant (dashed lines).

emphasized, for example, by Fischer *et al.*,[17] it is preferable these days to interpolate the tabulated thermochemical data presented in a fine grid rather than to use low-order polynomial expansions, and even a 25 K tabulation is sufficient for most partition functions.

3.1. The partition function

What the dimensionless partition function tells us is basically the ratio of the total number of "particles" to the number of "particles" in the ground state. Thus, the partition function provides a greatly simplified measure of how the particles are partitioned among the available energy levels. The magnitude of the partition function depends upon the magnitude of the fractional populations, and the latter depend both on the relative energy of the state and the chosen temperature. The largest value of the partition function can be very large but not infinite if the system contains a finite number of "particles". As seen in Table 2, $Q_{\text{int}}(T)$ of $H_2{}^{16}O$ becomes large as the temperature increases, reaching about (1200, 5300, 16 000, 40 000, 87 000, 170 000) at temperatures of (1000, 2000, 3000, 4000, 5000, 6000) K.

3.2. Comparison with previous results

The simplest way to approximate the partition function is through the application of the rigid-rotor and harmonic-oscillator (RRHO) model. For the RRHO model, an analytical formula is known for generating the partition function. Using experimental spectroscopic constants (A = 835 839.9 MHz, B = 435 354.5 MHz, and C = 278 133.3 MHz from Ref. 66; ν_1 = 3657.053 251 cm^{-1}, ν_2 = 1594.746 292 cm^{-1}, and ν_3 = 3755.928 548 cm^{-1} from Ref. 48), the temperature-dependent internal partition function can easily be computed. Figure 6 shows the differences for $Q_{\text{int}}(T)$ and $C_p(T)$ between the "exact" values of this study and those of the "analytical" RRHO partition function. Although the difference between

TABLE 2. The temperature-dependent internal partition functions of *ortho*- and *para*-$H_2{}^{16}O$, $Q_{int}^{ortho}(T)$, and $Q_{int}^{para}(T)$, respectively, and their first two moments, Q' and Q''. The same data are also presented for the nuclear-spin-equilibrated quantity $Q_{int}(T)$. Numbers in parentheses are the approximate two standard deviation uncertainties in the last digits of the $Q_{int}(T)$, $Q'_{int}(T)$, and $Q''_{int}(T)$ data

T/K	$Q_{int}^{para}(T)$	$Q'^{para}_{int}(T)$	$Q''^{para}_{int}(T)$	$Q_{int}^{ortho}(T)$	$Q'^{ortho}_{int}(T)$	$Q''^{ortho}_{int}(T)$	$Q_{int}(T)$	$Q'_{int}(T)$	$Q''_{int}(T)$
100	8.788 55	12.796 49	31.8905	26.364 58	38.400 31	95.5838	35.153 12(6)	51.196 80(5)	127.4743(1)
200	24.353 8	36.097 5	90.3065	73.061 3	108.292 6	270.9194	97.415 1(1)	144.390 1(1)	361.2259(3)
300	44.530 1	66.595 8	168.2010	133.590 4	199.787 5	504.603	178.120 6(2)	266.383 3(2)	672.8040(6)
400	68.642 3	104.049 2	268.974	205.926 9	312.147 5	806.921	274.569 2(3)	416.196 6(4)	1 075.895(1)
500	96.582 5	149.510 4	399.179	289.747 5	448.531 2	1 197.536	386.330 0(4)	598.041 7(6)	1 596.715(2)
600	128.540 1	204.420 2	565.317	385.620 4	613.260 4	1 695.952	514.160 5(5)	817.680 6(8)	2 261.269(3)
700	164.851 6	270.371	774.746	494.554 8	811.114	2 324.238	659.406 5(6)	1 081.485(1)	3 098.984(4)
800	205.945	349.173	1 036.321	617.835	1 047.518	3 108.963	823.780 1(8)	1 396.690(2)	4 145.284(5)
900	252.325	442.889	1 360.220	756.976	1 328.668	4 080.66	1 009.301(1)	1 771.558(2)	5 440.879(7)
1000	304.568	553.832	1 757.64	913.705	1 661.495	5 272.91	1 218.273(1)	2 215.327(3)	7030.54(1)
1100	363.316	684.527	2 240.64	1 089.948	2 053.581	6 721.91	1 453.264(2)	2 738.107(4)	8962.55(1)
1200	429.272	837.702	2 822.18	1 287.815	2 513.107	8 466.54	1 717.087(2)	3 350.809(5)	11 288.73(2)
1300	503.196	1 016.28	3 516.21	1 509.587	3 048.84	10 548.61	2 012.783(2)	4 065.120(6)	14 064.82(2)
1400	585.903	1 223.381	4 337.74	1 757.710	3 670.141	13 013.2	2 343.613(3)	4 893.522(7)	17 350.94(4)
1500	678.263	1 462.334	5 303.00	2 034.789	4 387.001	15 908.99	2 713.052(3)	5 849.335(9)	21 211.99(5)
1600	781.198	1 736.69	6 429.52	2 343.593	5 210.07	19 288.55	3 124.790(4)	6 946.76(1)	25 718.07(8)
1700	895.684	2 050.24	7 736.2	2 687.053	6 150.72	23 208.6	3 582.737(5)	8 200.96(2)	30 944.8(1)
1800	1 022.756	2 407.02	9 243.4	3 068.268	7 221.04	27 730.1	4 091.024(6)	9 628.06(3)	36 973.5(2)
1900	1 163.504	2 811.31	10 973.0	3 490.511	8 433.94	32 918.9	4 654.015(7)	11 245.25(4)	43 891.8(3)
2000	1 319.078	3 267.71	12 948.5	3 957.232	9 803.12	38 845.3	5 276.309(9)	13 070.83(5)	51 793.8(4)
2100	1 490.69	3 781.06	15 195.0	4 472.07	11 343.16	45 585.0	5 962.76(1)	15 124.22(7)	60 780.0(6)
2200	1 679.61	4 356.5	17 739.6	5 038.84	13 069.6	53 218.7	6 718.46(2)	17 426.1(1)	70 958.3(8)
2300	1 887.20	4 999.6	20 611	5 661.58	14 998.7	61 833	7 548.78(2)	19 998.3(1)	82 444(1)
2400	2 114.84	5 716.0	23 840	6 344.52	17 148.1	71 519	8 459.37(3)	22 864.1(2)	95 359(1)
2500	2 364.04	6 512.0	27 459	7 092.10	19 536.0	82 376	9 456.14(4)	26 048.0(2)	109 835(2)
2600	2 636.33	7 394.0	31 503	7 908.99	22 181.9	94 508	10 545.33(5)	29 575.9(3)	126 011(2)
2700	2 933.36	8 368.9	36 009	8 800.08	25 106.6	108 025	11 733.44(6)	33 475.4(4)	144 034(3)
2800	3 256.83	9 443.9	41 015	9 770.49	28 331.5	123 045	13 027.32(8)	37 775.4(5)	164 061(4)
2900	3 608.54	10 626.6	46 564	10 825.59	31 879.7	139 693	14 434.12(9)	42 506.3(6)	186 257(5)
3000	3 990.3	11 925.1	52 700	11 971.0	35 775.1	158 099	15 961.3(1)	47 700.2(8)	210 798(6)
3100	4 404.2	13 347.8	59 467	13 212.6	40 043.2	178 401	17 616.8(1)	53 391(1)	237 868(9)
3200	4 852.2	14 904	66 915	14 556.5	44 710	200 744	19 408.7(2)	59 614(1)	267 659(14)
3300	5 336.4	16 602	75 094	16 009.2	49 805	225 282	21 345.6(2)	66 406(2)	300 376(22)
3400	5 859.1	18 452	84 057	17 577.3	55 355	252 171	23 436.4(3)	73 807(2)	336 229(37)
3500	6 422.6	20 464	93 860	19 267.8	61 393	281 578	25 690.4(3)	81 857(4)	375 438(60)
3600	7 029.3	22 649	104 558	21 087.9	67 948	313 673	28 117.2(5)	90 598(5)	418 231(95)
3700	7 681.8	25 018	116 211	23 045.2	75 055	348 633	30 727.0(6)	100 074(9)	464 844(150)
3800	8 382.6	27 583	128 880	25 147.6	82 748	386 639	33 530.1(9)	110 330(13)	515 519(231)
3900	9 134	30 354	142 626	27 403	91 061	427 877	36 538(1)	121 415(20)	570 503(347)
4000	9 940	33 344	157 514	29 820	100 033	472 541	39 760(2)	133 377(30)	630 055(519)
4100	10 803	36 567	173 605	32 408	109 700	520 816	43 210(3)	146 266(45)	694 421(751)
4200	11 725	40 034	190 969	35 175	120 100	572 907	46 899(4)	160 134(65)	763 876(1 081)
4300	12 710	43 758	209 664	38 130	131 275	628 991	50 840(6)	175 033(93)	838 655(1 507)
4400	13 761	47 755	229 766	41 284	143 264	689 298	55 045(8)	191 019(132)	919 065(2 103)
4500	14 882	52 036	251 336	44 645	156 109	754 007	59 527(12)	208 145(184)	1 005 342(2 883)
4600	16 075	56 617	274 434	48 225	169 851	823 301	64 300(17)	226 468(253)	1 097 735(3 874)
4700	17 345	61 512	299 137	52 034	184 534	897 411	69 378(23)	246 046(344)	1 196 548(5 176)
4800	18 694	66 734	325 519	56 081	200 202	976 557	74 775(31)	266 936(462)	1 302 076(6 882)
4900	20 126	72 299	353 641	60 379	216 897	1 060 923	80 505(42)	289 196(613)	1 414 564(9 055)
5000	21 646	78 222	383 513	64 938	234 665	1 150 541	86 584(57)	312 886(806)	1 534 055(11 566)
5100	23 257	84 516	415 277	69 769	253 549	1 245 833	93 026(75)	338 066(1050)	1 661 110(14 817)
5200	24 962	91 199	448 970	74 885	273 596	1 346 915	99 847(98)	364 794(1354)	1 795 885(18 823)
5300	26 765	98 283	484 755	80 296	294 850	1 454 269	107 062(127)	393 133(1731)	1 939 024(24 100)
5400	28 672	105 786	522 468	86 015	317 357	1 567 409	114 687(164)	423 142(2195)	2 089 877(29 895)
5500	30 685	113 721	562 432	92 054	341 163	1 687 302	122 739(209)	454 884(2761)	2 249 734(37 402)
5600	32 809	122 105	604 338	98 425	366 314	1 813 022	131 234(265)	488 418(3449)	2 417 360(45 318)
5700	35 047	130 952	648 770	105 141	392 856	1 946 321	140 188(333)	523 808(4276)	2 595 091(55 918)
5800	37 405	140 279	695 568	112 214	420 837	2 086 714	149 619(416)	561 115(5267)	2 782 281(68 522)
5900	39 886	150 100	744 478	119 657	450 301	2 233 449	159 543(515)	600 401(6446)	2 977 927(82 113)
6000	42 494	160 433	796 005	127 483	481 299	2 388 030	169 977(635)	641 731(7842)	3 184 035(98 690)

TABLE 3. Thermochemical functions of nuclear-spin-equilibrated $H_2{}^{16}O$. Numbers in parentheses are the approximate two standard deviation uncertainties in the last digit of the quoted value

	$C_p(T)$ / J K^{-1} mol^{-1}			$S(T)$ / J K^{-1} mol^{-1}			$H(T)$/kJ mol^{-1}		
T/K	This work	Ruscic[19]	VT[30]	This work[a]	Ruscic[19]	VT[30]	This work	Ruscic[19]	VT[30]
100	33.300 86(1)	33.301	33.301	152.382 63(7)	152.387	152.384	3.289 53(1)	3.290	3.289
200	33.350 53(1)	33.351	33.351	175.479 84(7)	175.484	175.481	6.621 99(1)	6.622	6.622
300	33.595 84(1)	33.596	33.596	189.036 14(7)	189.040	189.038	9.966 18(1)	9.966	9.966
400	34.262 08(1)	34.262	34.262	198.782 71(8)	198.787	198.784	13.355 74(1)	13.356	13.356
500	35.225 93(1)	35.226	35.226	206.527 94(8)	206.532	206.530	16.828 50(1)	16.829	16.829
600	36.324 71(1)	36.325	36.325	213.046 16(9)	213.050	213.048	20.405 29(1)	20.405	20.405
700	37.496 27(1)	37.496	–	218.732 82(9)	218.737	–	24.095 82(1)	24.096	–
800	38.723 98(1)	38.724	38.728	223.819 3(1)	223.823	223.822	27.906 42(1)	27.906	27.907
900	39.991 72(1)	39.99	–	228.453 3(1)	228.457	–	31.841 96(1)	31.842	–
1000	41.275 27(1)	41.269	41.287	232.733 2(1)	232.737	232.737	35.905 29(1)	35.905	35.907
1100	42.547 76(1)	42.529	–	236.727 1(1)	236.730	–	40.096 64(1)	40.095	–
1200	43.785 53(2)	43.739	43.809	240.482 6(1)	240.482	240.490	44.413 68(1)	44.409	44.419
1300	44.970 88(3)	44.872	–	244.034 5(1)	244.029	–	48.851 99(1)	48.840	–
1400	46.092 48(5)	45.909	46.124	247.408 7(2)	247.393	247.420	53.405 73(1)	53.380	53.417
1500	47.144 41(7)	46.835	47.177	250.625 0(2)	250.592	250.639	58.068 16(1)	58.018	58.082
1600	48.124 9(1)	–	48.157	253.699 3(2)	–	253.715	62.832 22(2)	–	62.850
1800	49.878 0(2)	–	49.904	259.471 5(4)	–	259.491	72.637 00(5)	–	72.660
2000	51.378 7(3)	–	51.394	264.806 4(6)	–	264.828	82.766 6(1)	–	82.794
2200	52.664 6(4)	–	52.668	269.765 1(9)	–	269.788	93.174 2(2)	–	93.204
2400	53.773 0(5)	–	53.766	274.396(1)	–	274.418	103.820 6(3)	–	103.850
2600	54.737 3(6)	–	54.724	278.739(2)	–	278.761	114.673 8(4)	–	114.701
2800	55.584 8(7)	–	55.571	282.827(2)	–	282.848	125.707 7(5)	–	125.732
3000	56.337(1)	–	56.326	286.689(3)	–	286.708	136.901 3(7)	–	136.923
3200	57.008(4)	–	57.005	290.346(4)	–	290.365	148.237(1)	–	148.257
3400	57.608(9)	–	57.614	293.821(7)	–	293.840	159.700(2)	–	159.720
3600	58.14(2)	–	58.152	297.13(1)	–	297.149	171.276(5)	–	171.298
3800	58.60(4)	–	58.613	300.28(3)	–	300.305	182.950(9)	–	182.976
4000	58.98(7)	–	58.986	303.30(5)	–	303.322	194.71(2)	–	194.737
4200	59.3(1)	–	59.259	306.19(9)	–	306.207	206.54(4)	–	206.564
4400	59.5(2)	–	59.418	308.9(2)	–	308.968	218.41(7)	–	218.433
4600	59.6(4)	–	59.451	314.1(4)	–	311.610	242.2(2)	–	230.322
4800	59.6(5)	–	59.350	315.4(5)	–	314.139	248.2(2)	–	242.205
5000	59.5(6)	–	59.111	316.6(6)	–	316.557	254.2(3)	–	254.053
5200	59.3(8)	–	58.734	318.9(9)	–	318.868	266.0(4)	–	265.840
5400	59(1)	–	58.225	321(1)	–	321.076	277.9(6)	–	277.538
5600	59(1)	–	57.591	323(2)	–	323.182	289.7(9)	–	289.122
5800	58(2)	–	56.846	325(2)	–	325.191	301(1)	–	300.567
6000	58(2)	–	56.003	327(3)	–	327.104	313(2)	–	311.854

[a]The values reported in this column correspond to $S(T) - R \times \ln 4$, to make the $S(T)$ results of the present study approximately comparable to those of Refs. 19 and 30.

the exact and the RRHO values can be significant for $Q_{\text{int}}(T)$, especially at higher temperatures, considering the extreme simplicity of this model the agreement observed is quite pleasing for this semirigid molecule. Note also that most of the difference between the discrete, "exact" results and the continuous, "analytical" RRHO results at the lowest temperatures, below about 350 K, is due to failure of the integration approximation. The differences would tend toward zero if the experimental spectroscopic constants reported were used to generate rovibrational energy levels and these were used, via direct summation, for the computation of $Q_{\text{int}}(T)$. Note that, in a relative sense, the RRHO approximation seemingly works considerably better for $C_p(T)$ than for $Q_{\text{int}}(T)$.

TABLE 4. Coefficients of the fit, see Eq. (17), to the nuclear-spin-equilibrated internal partition function of $H_2{}^{16}O$

Coefficient	0–200 K	201–6000 K
a_0	0.000 041 414 5	86.911 235 747 2
a_1	5.266 826 868 3	−60.728 595 483 0
a_2	−8.443 870 982 4	15.444 769 415 1
a_3	4.977 715 050 4	−1.389 952 609 6
a_4	−1.344 986 784 2	−0.042 406 907 0
a_5	0.174 306 379 7	0.014 352 041 0
a_6	−0.008 793 622 9	−0.000 628 748 0

The left panel of Fig. 7 shows the comparison of our internal partition function with other high-temperature values by Harris *et al.*,[29] Irwin,[67] and VT.[30] The agreement with the VT results is especially pleasing. The right panel of Fig. 7 compares our $C_p(T)$ values with those of Harris *et al.*,[29] JANAF,[15] and VT.[30] As expected, the deviations here are slightly larger, but VT works very well below 4500 K.

3.3. NASA polynomials

The tabular form of thermochemical data used to be not very convenient for computerized applications. Thus, more

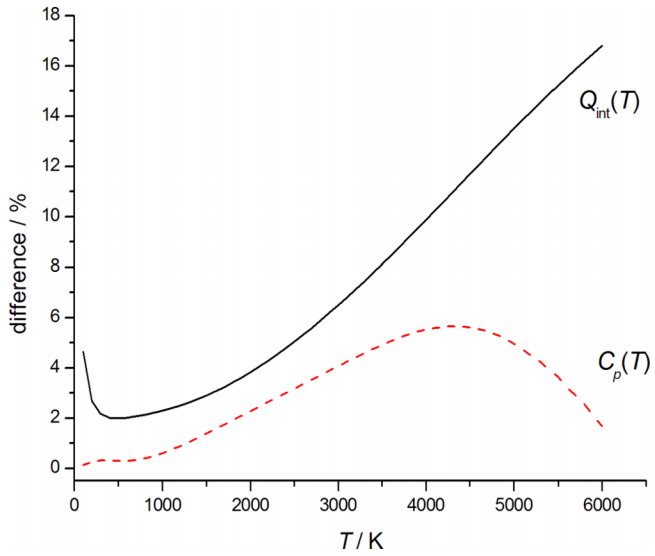

FIG. 6. Percentage difference between the "exact" values of $Q_{int}(T)$ and $C_p(T)$ and those corresponding to the "analytical" RRHO approximation. The apparent increase in the differences below 350 K for $Q_{int}(T)$ is due to the failure of approximating the direct sum with an integral when the density of states is low.

than four decades ago Gordon and McBride[68] suggested a set of low-order polynomials providing a convenient set of fit functions known as the older 7-constant and the newer 9-constant NASA polynomials. As Ruscic *et al.*[69] emphasized, (a) the 9-constant NASA polynomial reproduces the underlying data about two orders of magnitude better than the 7-constant NASA polynomial and (b) the thermochemical properties can be calculated in general with confidence in the fourth and fifth digit in the range of 150–3000 K. Nevertheless, the accuracy of even the 9-constant NASA polynomial is clearly insufficient when the data of the present study are considered. Therefore, thermochemical quantities determined in this study are provided in the supplementary material[35] at 1 K intervals. For those who need highly accurate thermochemical data, it is recommended to adapt the tabulated functions.

3.4. CODATA

The outstanding accuracy of the experimental (MARVEL) energy levels employed in this study means that all thermochemical quantities computed, especially at lower temperatures, have exceedingly high accuracy (the list of MARVEL rovibrational energies is complete up to 7500 cm^{-1}). One such quantity is $H^o(298.15\ K)–H^o(0\ K)$, the standard molar enthalpy increment (standard integrated heat capacity) of $H_2{}^{16}O$ between 298.15 and 0 K [$H^o(0\ K) = 0.0\ J\ mol^{-1}$]. This value is given for water in the official CODATA compilation[10] as $9.905 \pm 0.005\ kJ\ mol^{-1}$. Naturally, the value we compute, $9.904\,04 \pm 0.000\,01\ kJ\ mol^{-1}$, falls within the uncertainty of the old value, but it is more accurate by about two orders of magnitude. The newly determined value is insensitive to any reasonable change in the energy levels; the value is completely determined by energy levels lower than about 5000 cm^{-1}, and, notably, even the present first-principles PoKaZaTeL energy levels yield the same value though with higher uncertainty. While the present suggested change in the standard molar enthalpy increment of $H_2{}^{16}O$ is more or less inconsequential for most thermochemistry, as enthalpies of formation cannot be determined with this exceedingly small uncertainty, it nevertheless exemplifies the fact that it is more and more realistic to use high-resolution spectroscopic data to directly calculate thermodynamic quantities with minuscule uncertainties.

3.5. The low-temperature limit

Standard thermochemical textbooks and standard thermochemical tables found in various compendia[11,15] very rarely venture below 100 K. The reason is that there are special considerations about partition functions as well as thermochemical functions at the lowest temperatures, (well) below 100 K, due to the effect of nuclear spin statistics. It is only for higher temperatures that the *ortho* and *para* spin isomers of water are equilibrated, while in thermochemistry one always assumes an equilibrated mixture. In fact, the effect of nuclear spins can be investigated on effective structural parameters, as has been done for H_2O[70] and NH_3.[71]

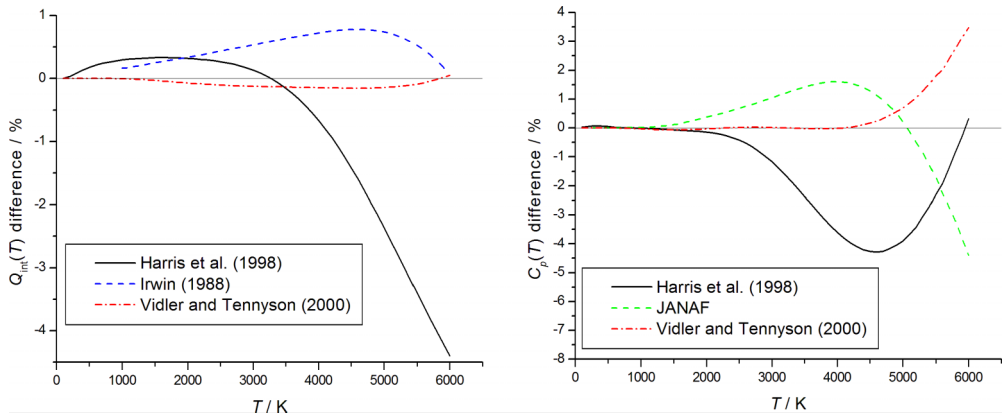

FIG. 7. Left panel: Comparison of the present $Q_{int}(T)$ values with those of Harris *et al.*,[29] Irwin,[67] and Vidler and Tennyson.[30] Right panel: Comparison of the present $C_p(T)$ values with those of Harris *et al.*,[29] JANAF,[15] and Vidler and Tennyson.[30]

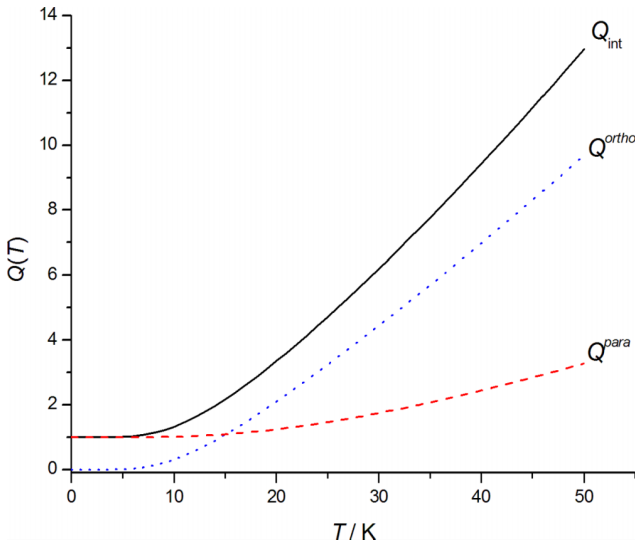

FIG. 8. The *ortho*-$H_2{}^{16}O$ (dotted, blue curve), the *para*-$H_2{}^{16}O$ (dashed, red curve), and the nuclear-spin-equilibrated $H_2{}^{16}O$ (full, black curve) partition functions at low temperatures, below 50 K.

Due to the distinct rovibrational states, the *ortho* and *para* species have slightly different effective structures and different thermochemical functions. The two nuclear-spin isomers can be in equilibrium (note again that this is what one always assumes in thermochemistry), or, if their interconversion is kinetically hindered, they exist as a mixture corresponding to distinct nuclear spin temperatures.[72,73] The same phenomenon is well known and has been studied[74,75] at the dawn of quantum mechanics for the H_2 molecule.

Figure 8 shows the values of the internal partition functions of the *ortho* and *para* spin isomers of $H_2{}^{16}O$ below 50 K. The different low-temperature behavior of $Q_{\rm int}^{ortho}$ and $Q_{\rm int}^{para}$ is evident from the figure. As mentioned, it is only the nuclear-spin-equilibrated $Q_{\rm int}$ (T) which is part of traditional thermochemistry. The reader should also be warned that one should not mix thermochemical data adhering to different

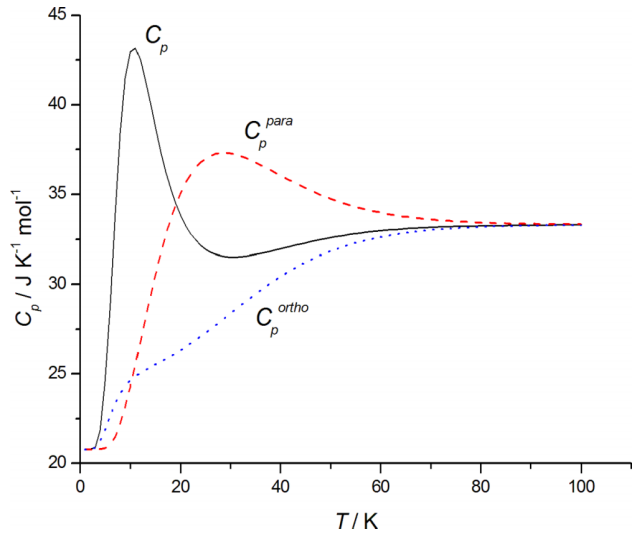

FIG. 9. The *ortho*-$H_2{}^{16}O$ (dotted, blue curve), the *para*-$H_2{}^{16}O$ (dashed, red curve), and the nuclear-spin-equilibrated $H_2{}^{16}O$ (full, black curve) isobaric heat capacities at low temperatures, below 100 K.

definitions, in this case the convention used to represent whether nuclear spin effects are considered or not.

Figure 9 shows the isobaric heat capacity of the *ortho* and *para* spin isomers as a function of temperature, as well as that of the equilibrium mixture. It is seen that up to 80 K the two water isomers possess rather different curves, but above 100 K the two curves become basically the same.

It must also be noted that the ortho-to-para (OPR) ratio is a useful diagnostic tool in astrochemistry.[76] The drastically different isobaric heat capacity of *ortho*- and *para*-$H_2{}^{16}O$ between 10 and 60 K computed here with high accuracy may have important consequences for certain applications.

4. Summary and Conclusions

The ideal-gas internal partition functions determined in this study for *ortho*-H_2O, *para*-H_2O, and their nuclear-spin-equilibrated mixture, in the temperature range of 0–6000 K, are the most accurate ones produced to date. The partition functions as well as the subsequently determined thermochemical functions, including the enthalpy, the entropy, and the isobaric heat capacity, have their own temperature-dependent uncertainties. All these thermochemical quantities are listed in 100 K increments in the main text and in 1 K increments in the supplementary material;[35] the latter should support several modeling applications. The accuracy of the present data is due to the following characteristics of this study:

(1) The internal partition function $Q_{\rm int}(T)$ and its first two moments are determined via the explicit summation technique; thus, their determination involves no modeling assumptions beyond the bare basics, distinguishing this study from almost all previous efforts.
(2) A large number of highly accurate, experimental rovibrational energy levels determined previously[48] is utilized; the list of experimental levels is complete up to 7500 cm^{-1}, significantly lowering the uncertainty of $Q_{\rm int}(T)$ below about 1000 K.
(3) At higher temperatures, between about 1000 and 3000 K, the completeness of the energy level set determines the true accuracy of the thermochemical quantities determined. We utilized the complete set of bound rovibrational energy levels of $H_2{}^{16}O$ obtained from a first-principles variational nuclear motion computation involving an exact kinetic energy operator and a highly accurate empirical PES.[36] Altogether, close to one million bound energy levels are utilized in this study.
(4) In order to ensure accuracy between 3000 and 6000 K, the contribution due to unbound states is considered via a simple model computation. Our test computations show that for $H_2{}^{16}O$ the contribution from the excited electronic states can be safely neglected.

Although in this study highly accurate thermochemical functions have been obtained for *ortho*- and *para*-$H_2{}^{16}O$, it is not yet common to include nuclear-spin statistical factors in the computation of partition functions and the related thermochemical functions. Thus, these data should be used

with caution in chemical reactions where nuclear spin effects are neglected for the other species involved. Nevertheless, it is expected that such data, especially important at low temperatures, will become available for a growing number of chemical species.

The accuracy of the reproduction of the present data with the 7- and 9-constant NASA polynomials is orders of magnitude worse than the internal accuracy of our results. Thus, it is recommended to use the 1 K list of computed values in all applications requiring high accuracy.

It is recommended that the new, exceedingly accurate value of the standard molar enthalpy increment (integrated heat capacity) of $H_2{}^{16}O$, $H^o(298.15\ K) = 9.904\,04(1)$ kJ mol^{-1}, should replace the value advocated in the CODATA compilation,[10] 9.905 ± 0.005 kJ mol^{-1}.

Finally, we note that the present procedure and data serve well the mission of IAPWS to determine accurate ideal- and real-gas data for water. For this task we need similarly high-quality data for all water isotopologues present in Vienna Standard Mean Ocean Water (VSMOW),[77–79] providing the isotopic composition[78] of the so-called "ordinary water substance." Work in this direction is in progress.

Acknowledgments

The authors are grateful to the COST action "Molecules in Motion" (MOLIM, CM1405) for support. A.G.C. thanks the NKFIH (Grant Nos. NK83583 and K119658) for supporting the work performed in Hungary. J.H. acknowledges support provided by the Czech Science Foundation (Grant No. 16-02647S). A.A.K. and N.F.Z. thank the Russian Fund for Basic Research for support. The authors are indebted to Professor Roberto Marquardt and Professor Branko Ruscic for their useful comments on certain aspects of this study.

5. References

[1]P. F. Bernath, Phys. Chem. Chem. Phys. **4**, 1501 (2002).
[2]N. F. Zobov, S. V. Shirin, R. I. Ovsyannikov, O. L. Polyansky, R. J. Barber, J. Tennyson, P.-F. Coheur, P. F. Bernath, M. Carleer, and R. Colin, Mon. Not. R. Astron. Soc. **387**, 1093 (2008).
[3]O. L. Polyansky, N. F. Zobov, I. I. Mizus, L. Lodi, S. N. Yurchenko, J. Tennyson, A. G. Császár, and O. V. Boyarkin, Philos. Trans. R. Soc., A **370**, 2728 (2012).
[4]D. L. Baulch, C. J. Cobos, R. A. Cox, P. Frank, G. Hayman, T. Just, J. A. Kerr, T. Murrells, M. J. Pilling, J. Troe, R. W. Walker, and J. Warnatz, J. Phys. Chem. Ref. Data **23**, 847 (1994).
[5]A. Burcat, "Third millennium ideal gas and condensed phase thermochemical database for combustion," TAE Report No. 867, Technion, Haifa, 2001.
[6]G. N. Lewis, M. Randall, K. S. Pitzer, and L. Brewer, *Thermodynamics* (McGraw-Hill, New York, 1961).
[7]J. D. Cox, Pure Appl. Chem. **54**, 1239 (1982).
[8]D. F. McMillan and D. M. Golden, Annu. Rev. Phys. Chem. **33**, 493 (1982).
[9]M. W. Chase, C. A. Davies, J. R. Downey, Jr., D. A. Frurip, R. A. McDonald, and A. N. Syverud, *JANAF Thermochemical Tables*, 3rd Ed., J. Phys. Chem. Ref. Data, Vol. 14, Suppl. 1 (1985).
[10]J. D. Cox, D. D. Wagman, and V. A. Medvedev, *CODATA Key Values for Thermodynamics* (Hemisphere, New York, 1989).
[11]L. V. Gurvich, I. V. Veyts, and C. B. Alcock, *Thermodynamic Properties of Individual Substances* (Hemisphere, New York, 1989).
[12]J. B. Pedley, *Thermochemical Data and Structures of Organic Compounds* (Thermodynamics Research Center, College Station, TX, 1994), Vol. 1.
[13]J. Berkowitz, G. B. Ellison, and D. Gutman, J. Phys. Chem. **98**, 2744 (1994).
[14]W. Wagner, J. R. Cooper, A. Dittmann, J. Kijima, H. Kretzschmar, A. Kruse, R. Mares, K. Oguchi, H. Sato, I. Stocker, O. Sifner, Y. Takaishi, I. Tanishita, J. Trubenbach, and T. Willkommen, J. Eng. Gas Turbines Power **122**, 150 (2000).
[15]M. W. Chase, Jr., *NIST-JANAF Thermochemical Tables*, 4th Ed., Journal of Physical and Chemical Reference Data Monograph No. 9 (American Institute of Physics, 1998).
[16]W. Wagner and A. Pruss, J. Phys. Chem. Ref. Data **31**, 387 (2002).
[17]J. Fischer, R. R. Gamache, A. Goldman, L. S. Rothman, and A. Perrin, J. Quant. Spectrosc. Radiat. Transfer **82**, 401 (2003).
[18]J. Tennyson, S. N. Yurchenko, A. F. Al-Refaie, E. J. Barton, K. L. Chubb, P. A. Coles, S. Diamantopoulou, M. N. Gorman, C. Hill, A. Z. Lam, L. Lodi, L. K. McKemmish, Y. Na, A. Owens, O. L. Polyansky, T. Rivlin, C. Sousa-Silva, D. S. Underwood, A. Yachmenev, and E. Zak, J. Mol. Spectrosc. **372**, 73 (2016).
[19]B. Ruscic, J. Phys. Chem. A **117**, 11940 (2013).
[20]J. E. Mayer and M. G. Mayer, *Statistical Mechanics* (Wiley, New York, 1940).
[21]D. A. McQuarrie, *Statistical Mechanics* (University Science Books, Sausalito, 2000).
[22]A. F. Krupnov, Phys. Rev. A **82**, 036703 (2010).
[23]K. K. Irikura, *Essential Statistical Thermodynamics* (American Chemical Society, Washington, DC, 1998).
[24]A. L. L. East and L. Radom, J. Chem. Phys. **106**, 6655 (1997).
[25]R. B. McClurg, R. C. Flagan, and W. A. Goddard III, J. Chem. Phys. **106**, 6675 (1997).
[26]P. Y. Ayala and H. B. Schlegel, J. Chem. Phys. **108**, 2314 (1998).
[27]O. L. Polyansky, A. G. Császár, S. V. Shirin, N. F. Zobov, P. Barletta, J. Tennyson, D. W. Schwenke, and P. J. Knowles, Science **299**, 539 (2003).
[28]J. M. L. Martin, J. P. Francois, and R. Gijbels, J. Chem. Phys. **96**, 7633 (1992).
[29]G. J. Harris, S. Viti, H. Y. Mussa, and J. Tennyson, J. Chem. Phys. **109**, 7197 (1998).
[30]M. Vidler and J. Tennyson, J. Chem. Phys. **113**, 9766 (2000).
[31]C. C. Stephenson and H. O. McMahon, J. Chem. Phys. **7**, 614 (1939).
[32]R. Q. Topper, Q. Zhang, Y. P. Liu, and D. G. Truhlar, J. Chem. Phys. **98**, 4991 (1993).
[33]F. V. Prudente and A. J. C. Varandas, J. Phys. Chem. A **106**, 6193 (2002).
[34]L. Gurvich, I. V. Veyts, C. B. Alcock, and V. S. Iorish, *Thermodynamic Properties Of Individual Substances: Elements and Compounds*, 4th ed. (Hemisphere, New York, 1991), Vol. 5.
[35]See supplementary material at http://dx.doi.org/10.1063/1.4967723 for listings of various temperature-dependent thermochemical quantities, both with and without estimated contributions for unbound states.
[36]O. L. Polyansky, A. A. Kyuberis, N. Zobov, J. Tennyson, L. Lodi, and S. N. Yurchenko, "ExoMol molecular line lists XXII: a complete line list for water," Mon. Not. R. Astron. Soc. (unpublished).
[37]R. J. Barber, J. Tennyson, G. J. Harris, and R. N. Tolchenov, Mon. Not. R. Astron. Soc. **368**, 1087 (2006).
[38]J. Tennyson, N. F. Zobov, R. Williamson, O. L. Polyansky, and P. F. Bernath, J. Phys. Chem. Ref. Data **30**, 735 (2001).
[39]S. Viti, J. Tennyson, and O. L. Polyansky, Mon. Not. R. Astron. Soc. **287**, 79 (1997).
[40]S. Viti, "Infrared spectra of cool stars and sunspots," Ph.D. thesis, University of London, 1997.
[41]H. Y. Mussa and J. Tennyson, J. Chem. Phys. **109**, 10885 (1998).
[42]T. Szidarovszky and A. G. Császár, J. Chem. Phys. **142**, 014103 (2015).
[43]N. F. Zobov, S. V. Shirin, L. Lodi, B. C. Silva, J. Tennyson, A. G. Császár, and O. L. Polyansky, Chem. Phys. Lett. **507**, 48 (2011).
[44]T. Szidarovszky and A. G. Császár, Mol. Phys. **111**, 2131 (2013).
[45]A. G. Császár, G. Czakó, T. Furtenbacher, and E. Mátyus, Annu. Rep. Comput. Chem. **3**, 155 (2007).
[46]T. Furtenbacher, A. G. Császár, and J. Tennyson, J. Mol. Spectrosc. **245**, 115 (2007).
[47]T. Furtenbacher and A. G. Császár, J. Quant. Spectrosc. Radiat. Transfer **113**, 929 (2012).
[48]J. Tennyson, P. F. Bernath, L. R. Brown, A. Campargue, M. R. Carleer, A. G. Császár, L. Daumont, R. R. Gamache, J. T. Hodges, O. V. Naumenko, O. L. Polyansky, L. S. Rothmam, A. C. Vandaele, N. F. Zobov, A. R. Al Derzi, C. Fábri, A. Z. Fazliev, T. Furtenbacher, I. E. Gordon, L. Lodi, and I. I. Mizus, J. Quant. Spectrosc. Radiat. Transfer **117**, 29 (2013).

[49]J. Tennyson, P. F. Bernath, L. R. Brown, A. Campargue, M. R. Carleer, A. G. Császár, R. R. Gamache, J. T. Hodges, A. Jenouvrier, O. V. Naumenko, O. L. Polyansky, L. S. Rothman, R. A. Toth, A. C. Vandaele, N. F. Zobov, L. Daumont, A. Z. Fazliev, T. Furtenbacher, I. E. Gordon, S. N. Mikhailenko, and S. V. Shirin, J. Quant. Spectrosc. Radiat. Transfer **110**, 573 (2009).
[50]J. Tennyson, P. F. Bernath, L. R. Brown, A. Campargue, M. R. Carleer, A. G. Császár, L. Daumont, R. R. Gamache, J. T. Hodges, O. V. Naumenko, O. L. Polyansky, L. S. Rothman, R. A. Toth, A. C. Vandaele, N. F. Zobov, A. Z. Fazliev, T. Furtenbacher, I. E. Gordon, S. N. Mikhailenko, and B. A. Voronin, J. Quant. Spectrosc. Radiat. Transfer **111**, 2160 (2010).
[51]J. Tennyson, P. F. Bernath, L. R. Brown, A. Campargue, A. G. Császár, L. Daumont, R. R. Gamache, J. T. Hodges, O. V. Naumenko, O. L. Polyansky, L. S. Rothmam, A. C. Vandaele, N. F. Zobov, N. Dénes, A. Z. Fazliev, T. Furtenbacher, I. E. Gordon, S.-M. Hu, T. Szidarovszky, and I. A. Vasilenko, J. Quant. Spectrosc. Radiat. Transfer **142**, 93 (2014).
[52]J. Tennyson, P. F. Bernath, L. R. Brown, A. Campargue, A. G. Császár, L. Daumont, R. R. Gamache, J. T. Hodges, O. V. Naumenko, O. L. Polyansky, L. S. Rothman, A. C. Vandaele, and N. F. Zobov, Pure Appl. Chem. **86**, 71 (2014).
[53]A. G. Császár and T. Furtenbacher, J. Mol. Spectrosc. **266**, 99 (2011).
[54]H. W. Kroto, *Molecular Rotation Spectra* (Dover, New York, 1992).
[55]A. G. Császár, C. Fábri, T. Szidarovszky, E. Mátyus, T. Furtenbacher, and G. Czakó, Phys. Chem. Chem. Phys. **13**, 1085 (2012).
[56]P. Barletta, S. V. Shirin, N. F. Zobov, O. L. Polyansky, J. Tennyson, E. F. Valeev, and A. G. Császár, J. Chem. Phys. **125**, 204307 (2006).
[57]J. Tennyson, M. A. Kostin, P. Barletta, G. J. Harris, O. L. Polyansky, J. Ramanlal, and N. F. Zobov, Comput. Phys. Commun. **163**, 85 (2004).
[58]O. V. Boyarkin, M. A. Koshelev, O. Aseev, P. Maksyutenko, T. R. Rizzo, N. F. Zobov, L. Lodi, J. Tennyson, and O. L. Polyansky, Chem. Phys. Lett. **568-569**, 14 (2013).
[59]P. J. Mohr, D. B. Newell, and B. N. Taylor, Rev. Mod. Phys. **88**, 035009 (2016).
[60]http://www.ciaaw.org/, 2016.
[61]T. Szidarovszky, A. G. Császár, and G. Czakó, Phys. Chem. Chem. Phys. **12**, 8373 (2010).
[62]F. H. Mies and P. S. Julienne, J. Chem. Phys. **77**, 6162 (1982).
[63]N. Graham, M. Quandt, and H. Weigel, Lect. Notes Phys. **777**, 15 (2009).
[64]H. Chung, B. J. Braams, K. Bartschat, A. G. Császár, G. Drake, T. Kirchner, V. Kokoouline, and J. Tennyson, J. Phys. D: Appl. Phys. **49**, 363002 (2016).
[65]J. J. Munro, J. Ramanlal, and J. Tennyson, New J. Phys. **7**, 196 (2005).
[66]A. G. Császár, G. Czakó, T. Furtenbacher, J. Tennyson, V. Szalay, S. V. Shirin, N. F. Zobov, and O. L. Polyansky, J. Chem. Phys. **122**, 214305 (2005).
[67]A. W. Irwin, Astron. Astrophys., Suppl. Ser. **74**, 145 (1988).
[68]B. J. McBride and S. Gordon, Computer Program for Calculating and Fitting Thermodynamic Functions, NASA RP-1271, 1992.
[69]B. Ruscic, J. E. Boggs, A. Burcat, A. G. Császár, J. Demaison, R. Janoschek, J. M. L. Martin, M. L. Morton, M. J. Rossi, J. F. Stanton, P. G. Szalay, P. R. Westmoreland, F. Zabel, and T. Bérces, J. Phys. Chem. Ref. Data **34**, 573 (2005).
[70]G. Czakó, E. Mátyus, and A. G. Császár, J. Phys. Chem. A **113**, 11665 (2009).
[71]I. Szabó, C. Fábri, G. Czakó, E. Mátyus, and A. G. Császár, J. Phys. Chem. A **116**, 4356 (2012).
[72]N. Dello Russo, M. A. DiSanti, K. Magee-Sauer, E. L. Gibb, M. J. Mumma, R. J. Barber, and J. Tennyson, Icarus **168**, 186 (2004).
[73]N. Dello Russo, B. P. Bonev, M. A. DiSanti, E. L. Gibb, M. J. Mumma, K. Magee-Sauer, R. J. Barber, and J. Tennyson, Astrophys. J. **621**, 537 (2005).
[74]D. M. Dennison, Proc. R. Soc. A **115**, 483 (1927).
[75]K. F. Bonhoeffer and P. Harteck, Z. Physik. Chem. **4B**, 113 (1929).
[76]K. Furuya, Y. Aikawa, U. Hincelin, G. E. Hassel, E. A. Bergin, A. I. Vasyunin, and E. Herbst, Astron. Astrophys. **584**, A124 (2015).
[77]R. Gonfiantini, Nature **271**, 534 (1978).
[78]National Institute of Standards and Technology, Report of Investigation, Reference Materials 8535, 8536, and 8537, 2005.
[79]National Institute of Standards and Technology, Report of Investigation, Reference Material 8535a, 2011.